

Geochemical constraints on the petrogenesis of Pan-African A-type granites in the Damara Belt, Namibia

F. McDermott¹, N.B.W. Harris² and C.J. Hawkesworth³

¹Department of Geology, University College Dublin, Belfield, Dublin 4, Ireland.

²Department of Earth Sciences, The Open University, Walton Hall, Milton Keynes, MK7 6AA, U.K.

³Department of Earth Sciences, Bristol University, Bristol BS8 1RJ, U.K.

This paper presents major element, trace element and radiogenic isotope data for selected A-type granites (*sensu-lato*) from the Pan-African Damara belt, Namibia. The granites studied include those from Sorris-Sorris, Dachsberg, Horebis River, and a Salem-type intrusion from the Swakopmund region. The first three of these exhibit high $\text{FeO}/(\text{FeO} + \text{MgO})$ and high TiO_2/MgO ratios, characteristics of A-type granites, and all four intrusions display distinctive enrichments in the high field strength elements (e.g. Nb, Y, Zr). However, only a small number of the high-silica (>73 wt % SiO_2) samples exhibit low CaO and low Al_2O_3 , characteristics of many A-type granites world-wide. Magmatic temperatures inferred from the zirconium solubility model (typically in excess of 780°C) are higher than those of broadly contemporaneous S-type granites, although elevated F abundances, characteristic of many A-type granites, will result in a higher zirconium solubility at a given temperature. Most of the A-type granites studied here exhibit initial Sr and Nd isotope ratios similar to Damara calc-alkaline diorites and granodiorites. Their major and trace element characteristics are consistent with derivation by partial melting of felsic calc-alkaline source rocks, but less silicic examples require a contribution from more mafic material. On the basis of results from recently published melting experiments on felsic calc-alkaline sources, mid-crustal low-pressure (4-6 kbar) rather than high-pressure (10 kbar) melting is inferred. The generation of intraplate trace element signatures (high HFS/LILE ratios) by partial melting of calc-alkaline source rocks requires enhanced HFS element solubility in the magmas. This could reflect higher magmatic temperatures which promotes dissolution of HFS-enriched minor phases and/or high F activity in the magma. The data for these A-type granites preclude any significant involvement of old metasedimentary material in their genesis.

Introduction

The geochronology, geochemistry and petrogenesis of granites in the Pan-African Damara mobile belt have been the subject of numerous studies (Haack *et al.*, 1982; Hawkesworth and Marlow, 1983; Miller, 1983; McDermott *et al.*, 1996; Jung *et al.*, 1998). Several authors have highlighted the apparent absence of significant crustal growth (Hawkesworth *et al.*, 1981; 1983; Harris *et al.*, 1987, McDermott *et al.*, 1996). Here we focus on the geochemically distinct HFS element enriched granites (*sensu-lato*) which are equivalent to the group II Damara granites of McDermott *et al.* (1996). New major element, trace element and isotope data are presented for the Horebis River granite, the Sorris-Sorris granite, the Dachsberg granite and a Salem-type granite from the Swakopmund region (Fig. 1). In addition, recently published data for three A-type Damara granites (Jung *et al.*, 1998) from Oetmeod, Baukwab and Albrechtal (Fig. 1) are included for comparison.

While there is no generally accepted formal definition for A-type granites, there is wide agreement that they exhibit several distinctive geochemical characteristics. These include high total alkalis, high $\text{K}_2\text{O}/\text{Na}_2\text{O}$, high FeO/MgO , high TiO_2/MgO , high Ga/Al , high F contents and low Al_2O_3 , CaO, MgO, Sr and Eu contents relative to I-type suites of similar SiO_2 contents (Collins *et al.*, 1982; Whalen *et al.*, 1987; Patiño Douce, 1997). Typically A-type granites also exhibit high abundances of the high-field strength elements (e.g. Nb, Y, Zr). High magmatic temperatures ($>900^\circ\text{C}$) and low water contents (<2.5 wt. % H_2O) have been inferred from data on experimental charges (Clemens *et al.*, 1986) and natural samples (Creaser and White, 1991; Turner *et al.*, 1992).

Eby (1992) used trace elements (Nb, Y and Ce) to discriminate between so-called A_1 and A_2 types that

were interpreted as differentiates of magmas derived predominantly by partial melting of mantle and crustal sources respectively. The A_1 group is characterised by high Nb/Y ratios that reflect high Nb/Y ratios in their alkali basaltic parental magmas. These occur in rift environments. The A_2 group, by contrast, occurs in post-collisional or post-orogenic environments. These have lower Nb/Y ratios, typically between those of average continental crust and island-arc basalts (Eby, 1992).

Turner *et al.* (1992) developed the theme of a mantle source for some A-type suites and argued that A-type granites from the Padthaway Ridge, South Australia,

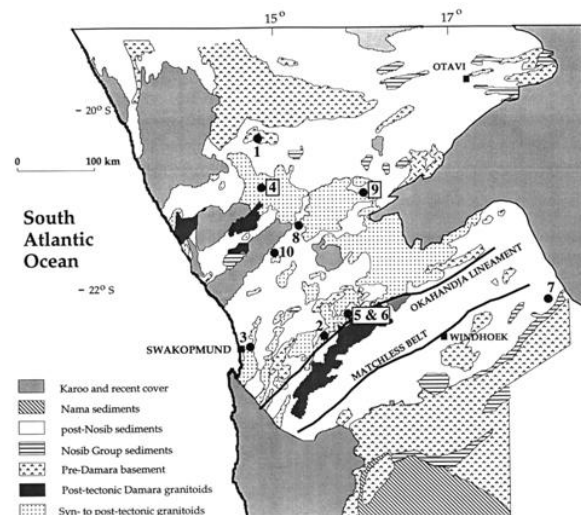


Figure 1: Simplified geological map of the Pan-African Damara Orogen of Namibia showing the distribution of the major rock types. The numbers denote the locations of the various granitoid intrusions referred to in the text: 2. Horebis River granite; 3. Swakopmund Salem-type granite; 4. Sorris-Sorris granite; 7. Dachsberg granite; 8. Baukwab granite; 9. Albrechtal granite; 10. Oetmeod granite.

represent fractionates of coeval mantle-derived basaltic parental magmas. This interpretation is strongly supported by their positive ϵ^{Nd}_t , low initial $^{87}Sr/^{86}Sr$ ratios and the occurrence of contemporaneous gabbros that contain A-type felsic rocks generated by fractional crystallisation. By contrast, in a study of predominantly peralkaline A-type granites in the Topsails igneous suite (Newfoundland), Whalen *et al.* (1996) argued that the major element, trace element and isotope data are best explained by re-melting of the lithospheric mantle, with only a limited role for fractional crystallisation. King *et al.* (1997) contended that metaluminous to weakly peraluminous A-type granites from the Lachlan Fold Belt (southeastern Australia) were derived by partial melting of felsic crustal sources and that aluminous types should be distinguished from predominantly peralkaline types in the A-type classification.

Three of the four granites discussed here are considered unequivocally to be A-type, namely those from Sorris-Sorris, Horebis River and Dachsberg. They are distinguished from the other Damara intrusions on the basis of their high TiO_2/MgO and high $FeO_t/(FeO_t + MgO)$ ratios relative to Damara leucogranites with similar silica contents. In a fourth intrusion, the Salem-type granite from Swakopmund, these characteristics are more weakly developed. All four granites exhibit strong HFS element enrichment.

Regional geological setting, petrography and geochronology

Regional geological setting

The Pan-African Damara Orogen comprises a north-south trending coastal branch and a north-east trending intracontinental branch (Martin and Porada, 1977). The orogen has been subdivided into several zones based on stratigraphy, structure, metamorphic grade, geochronology and aeromagnetic data (Miller, 1983). The Damara granites (*sensu lato*) range in age from 840–460 Ma and they crop out over a total area of at least 74,000 km², predominantly within a broad intracontinental orogenic belt that extends north-eastwards from Swakopmund (Fig. 1). Granite (*sensu stricto*) accounts for some 96% of the total granitoid outcrop and the remaining 4% is divided approximately equally between gabbro/diorite and tonalite/granodiorite associations (Miller, 1983). The predominance of granite (*sensu stricto*) over other granitoid types is in marked contrast to the dominance of tonalite-granodiorite compositions that characterises many destructive margin environments (e.g. Pitcher, 1979).

Field relationships and petrography

The Horebis River granite (Downing and Coward, 1981) pre-dates the regional D2 penetrative fabric and consists of quartz, K-feldspar, plagioclase, biotite and

muscovite with accessory apatite, sphene, monazite and zircon. The Sorris-Sorris granite is a late porphyritic alkaline granite which was intruded into the Omangambo pluton of Salem-type granite near the northern margin of the Damara belt (Miller, 1980) after the development of the regional penetrative fabric. It consists of quartz, K-feldspar, plagioclase (An_{12}), biotite and secondary muscovite. Accessory phases include zircon, apatite and monazite. The Dachsberg granite post-dates the regional tectonic fabric and forms a small plug-like intrusion on the southern margin of the orogen (Fig. 1) and consists almost entirely of quartz and K-feldspar with spectacular symplectitic intergrowths. The Salem-type granite that occurs 20 km east of Swakopmund (Fig. 1), hereafter referred to as the Swakopmund Salem-type granite, post-dates the main regional penetrative fabric in the region (Hawkesworth *et al.*, 1983). Unlike the other granites discussed here this granite does not strongly exhibit the major element characteristics of A-type granites (see below) but it is included in the discussion because it displays strong HFS element enrichment.

Geochronology

Samples from the Horebis River granite yield an eleven-point (M.S.W.D. = 11) Rb-Sr whole-rock isochron age of 633 ± 39 (2 σ) with a high initial $^{87}Sr/^{86}Sr$ ratio of 0.712 ± 6 (Downing and Coward, 1981). An eight-point Rb-Sr whole-rock isochron (M.S.W.D. = 4.3) for the Sorris-Sorris granite defines an age of 495 ± 15 Ma (2 σ) with an initial $^{87}Sr/^{86}Sr$ ratio of 0.709 ± 0.001 (Hawkesworth *et al.*, 1983). The Dachsberg granite yields a Rb-Sr whole-rock isochron age of 526 ± 5 Ma with an elevated initial Sr isotope ratio of 0.722 (Esquevin and Menendez, 1975). The Swakopmund Salem-type granite yields a six-point whole-rock Rb-Sr isochron (M.S.W.D. = 0.03) age of 563 ± 63 Ma (2 σ) with an initial $^{87}Sr/^{86}Sr$ ratio of 0.707 ± 4 (Hawkesworth *et al.*, 1983). The A-type granites from Baukwab, Albrechtstal and Oetmoed (Jung *et al.*, 1998) yielded Rb-Sr whole-rock ages of 507 ± 44 Ma (5 whole-rocks, M.S.W.D. = 3.05, initial $^{87}Sr/^{86}Sr = 0.70686$), 436 ± 58 Ma (5 whole-rocks, M.S.W.D. = 14.3, initial $^{87}Sr/^{86}Sr = 0.70897$) and 510 ± 48 Ma (6 whole-rocks, M.S.W.D. = 12, initial $^{87}Sr/^{86}Sr = 0.70725$) respectively. The age uncertainties were reduced by whole-grain (zircon, monazite, sphene) $^{207}Pb/^{206}Pb$ evaporation analyses to yield ages of between 521.8 ± 1 and 528.6 ± 1.1 Ma for Baukwab (zircon), 484 ± 2 to 488 ± 2.5 Ma for Albrechtstal (zircon), and 490.3 ± 1 (monazite) to 496.7 ± 3 Ma (sphene) for Oetmoed. A detailed discussion of these results and an account of the analytical techniques employed is given in Jung *et al.* (1998).

Major element data

The Damara A-type granitoids define a wide compo-

sitional range (61-76 wt% SiO₂). For comparison in Figure 2 we show the averages of major element analyses for well characterised A-type samples from the Topsails granite (Whalen *et al.*, 1987, 1996) and the Lachlan Fold Belt (White and Chappell, 1983; Turner *et al.*, 1992). These are relatively silicic (>73 wt.% SiO₂, arrows T and L). The three A-type Damara suites studied by Jung *et al.* (1998) from Albrechtstal, Oetmoed and Baukwab (localities 5-7, Fig. 1) include samples that

are less silicic (<67 wt.% SiO₂) than most of the granites for which new data are presented in Table 1.

Recently Patiño Douce (1997) drew attention to the high FeO_i/(FeO_t + MgO) and high TiO₂/MgO ratios that appear to characterise many A-type granite suites. The Damara A-type granites exhibit a range in FeO_i/(FeO_t + MgO) and TiO₂/MgO but it is noticeable that most have FeO_i/(FeO_t + MgO) and TiO₂/MgO ratios that are higher than those in Damara leucogranites and alaskites with similar silica contents (Figures 2a and 2b).

With the exception of the highest silica samples (from the Dachsberg and Horebis River granites), the Damara A-type granites do not exhibit the marked Al₂O₃ depletion that characterises typical average A-type granites from the Topsails suite or the Lachlan Fold Belt (e.g. Whalen *et al.*, 1987; Turner, 1992; T and L in Fig. 2c).

Low CaO is considered to be a characteristic of A-type granites (e.g. Whalen *et al.*, 1987) and CaO contents in the range 0.75-1.1 wt.% are typical for the Topsails and Lachlan Fold Belt A-type granites. In Figure 2d it is clear that the broad negative trend of the data for the Damara A-type granites encompass the average values for A-type granites from the Lachlan Fold Belt and the Topsails suite (L and T, Fig. 2d). High CaO contents in the Albrechtstal, Baukwab and Oetmoed suites (Jung *et al.*, 1998) reflect their lower silica contents. By contrast, the Dachsberg samples and most of the Horebis River samples have lower CaO contents than average A-types (Fig. 2d) reflecting their highly differentiated character. There is considerable overlap between the Damara A-type granites and Damara two-mica peraluminous S-type leucogranites (McDermott, 1996) on CaO vs. SiO₂ and Al₂O₃ vs. SiO₂ diagrams (not shown). There is, therefore, no strong evidence for CaO or Al₂O₃ depletion in the Damaran A-types relative to the S-type leucogranites.

Figure 3, a plot of molecular Al₂O₃/(Na₂O + K₂O) vs. Al₂O₃/(Na₂O + K₂O + CaO), highlights the wide range in major element compositions exhibited by the Damara

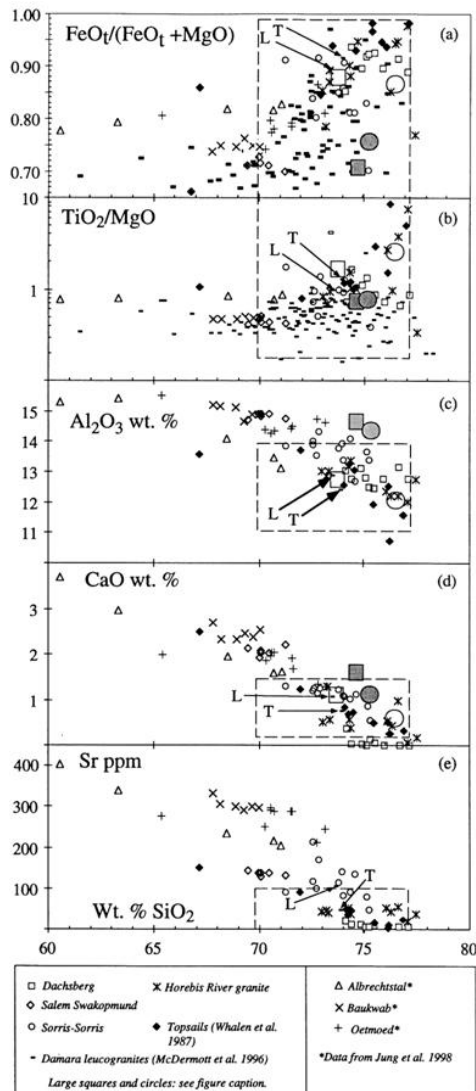


Figure 2: Selected major and trace element data plotted against silica contents. Also shown are average values for the Topsails A-type granite (T) and an average of A-type granites from the Lachlan Fold Belt (L) after Whalen *et al.* (1987) and Turner *et al.* (1992) respectively. Large rectangles with dashed-line outlines indicate the ± 1 standard deviation range on these averages. Results from experimental studies on dehydration melting of calc-alkaline rocks at 950°C (Patiño Douce, 1997) are shown as large squares and circles. Large squares represent compositions of experimental melts produced by melting of a tonalite at 4 kbar (open squares) and 8 kbar (stipple-filled squares). Large circles represent compositions of experimental melts produced by melting of a granodiorite at 4 kbar (open circles) and 8 kbar (stipple-filled circles).

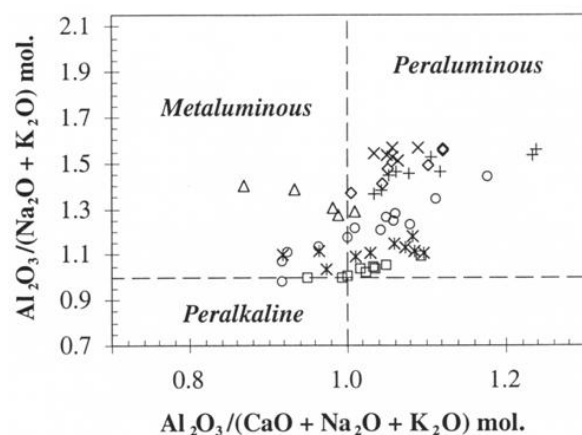


Figure 3: Molecular Al₂O₃/(Na₂O + K₂O) plotted against molecular Al₂O₃/(CaO + Na₂O + K₂O) to illustrate that the A-type granites discussed here are metaluminous to peraluminous. Data symbols as in Figure 2.

Table 1: Major and trace element data for selected HFSE-enriched Damara granitoids

	SiO ₂	TiO ₂	Al ₂ O ₃	Fe ₂ O ₃	MnO	MgO	CaO	Na ₂ O	K ₂ O	P ₂ O ₅	L.O.I.	Totals	Nb	Pb	Rb	Sr	Th	Y	Zr	Hf	Ta
Dachsberg granite																					
1012	74.9	0.27	13.11	2.30	0.01	0.24	0.02	4.16	5.35	0.08	0.52	100.96	54	10	218	11	15	57	316		
1013	75.12	0.28	12.8	2.58	0.01	0.21	0.01	4.38	5.22	0.10	0.37	101.08	55	9	197	7	6	70	310		
1014	74.41	0.25	12.77	2.46	0.01	0.15	0.02	4.34	5.15	0.13	0.50	100.19	55	10	205	11	14	60	287		
1015	74.14	0.26	13.02	2.30	0.02	0.36	0.37	4.62	5.01	0.27	0.57	100.94	59	11	220	21	31	90	332		
1030	75.51	0.13	12.46	2.07	0.01	0.15	0.06	3.89	5.12	0.40	0.38	100.18	85	10	146	8	22	108	378		
1031	77.13	0.13	12.77	1.33	0.01	0.15	0.01	6.02	2.36	0.05	0.47	100.43	71	8	54	6	22	105	367		
1032	75.96	0.11	12.76	1.43	0.01	0.15	0.01	5.48	2.88	0.04	0.66	99.49	18	4	12	395	3	25	174		
1034	76.67	0.10	13.16	1.78	0.01	0.15	0.01	4.28	4.60	0.05	0.50	101.31	75	10	110	7	16	58	381		
1035	75.28	0.13	12.49	2.01	0.01	0.15	0.13	4.38	4.47	0.04	0.45	99.54	78	10	106	7	16	116	441		
Horebis red granite																					
YC3	76.05	0.25	12.36	1.67	0.02	0.09	0.54	3.08	5.71	0.00	0.35	100.12	43	18	154	54	17	32	188		
YC1	77.05	0.23	12.04	1.49	0.00	0.03	0.07	2.36	6.44	0.00	0.51	100.12	86	73	212	21	32	39	236		
YC4	74.35	0.31	13.38	2.47	0.02	0.30	0.38	3.05	6.24	0.05	0.46	101.01	79	19	197	39	26	62	340		
YC5	73.19	0.37	12.87	2.14	0.03	0.52	1.30	3.20	5.92	0.00	1.12	100.66	89	21	158	47	26	67	370		
YC6	73.31	0.35	13.05	2.75	0.02	0.37	0.56	2.80	5.94	0.00	0.56	99.71	79	20	151	41	26	58	370		
YC8	77.48	0.11	12.77	1.19	0.00	0.32	0.18	3.37	5.45	0.00	0.42	101.29	100	21	122	37	40	54	221		
YC9	76.28	0.25	12.24	1.59	0.01	0.25	0.45	2.96	6.36	0.03	0.37	100.79	48	18	188	43	33	37	188		
YC10	74.28	0.36	13.19	2.34	0.02	0.23	0.57	3.27	5.58	0.00	0.51	100.35	72	22	124	52	18	55	326		
YC11	76.60	0.23	12.24	1.20	0.02	0.06	0.99	2.77	5.87	0.00	0.58	100.56	51	19	173	55	36	45	160		
YC12	72.98	0.34	13.05	2.62	0.01	0.40	0.53	2.96	6.34	0.00	0.51	99.74	77	18	169	45	29	58	382		
Sorris-Sorris granite																					
RM654	72.85	0.22	14.31	1.93	0.04	0.16	1.24	3.05	5.18	0.07	0.56	99.61	22	29	244	170	47	54	193		
RM662	72.59	0.28	14.01	2.16	0.03	0.29	1.24	2.94	5.65	0.00	0.51	99.70	20	31	219	213	50	31	250		
RM663	75.26	0.12	13.39	0.81	0.03	0.31	0.54	4.66	5.51	0.03	0.58	101.24	25	23	295	48	53	81	94	3.61	4.27
RM664	72.74	0.17	13.53	1.48	0.03	0.33	1.14	4.32	5.13	0.00	1.07	99.94	32	26	321	98	52	52	152	5.16	4.00
RM665	73.99	0.23	13.94	1.68	0.04	0.25	1.08	3.35	5.25	0.06	0.92	100.79	33	27	297	140	50	44	180		
RM666	73.78	0.27	13.78	1.71	0.03	0.27	1.22	2.74	5.91	0.14	0.54	100.39	44	24	261	115	47	63	194	6.52	3.27
RM667	71.26	0.40	13.85	2.64	0.04	0.23	1.30	2.88	6.12	0.04	1.07	99.83	62	22	301	92	52	53	323		
RM673	72.55	0.26	13.91	2.09	0.06	0.36	1.19	3.66	3.36	0.00	1.27	98.71	43	19	279	117	57	72	229	6.69	4.10
2198	75.15	0.13	13.67	0.97	0.03	0.18	0.85	3.63	4.75	0.06	0.98	100.40	47	31	204	79	20	68	108		
2199	74.05	0.19	13.38	1.64	0.02	0.15	1.07	3.74	4.86	0.09	1.06	100.25	60	35	210	83	29	80	131		
2200	74.34	0.16	14.08	1.15	0.02	0.24	1.02	3.75	5.06	0.09	0.90	100.81	55	39	205	90	27	75	127		
2204	74.59	0.36	12.70	1.90	0.05	0.40	1.11	3.22	5.42	0.04	0.57	100.36	60	21	216	134	60	64	225		
Swakopmund Salem-type granite																					
SM1	70.46	0.51	14.90	3.14	0.05	1.15	2.03	2.74	4.71	0.11	0.65	100.45	32	36	271	138	23	47	184		
SM2	71.24	0.48	14.75	2.95	0.05	1.14	2.20	3.46	3.99	0.12	0.97	101.35	29	36	186	132	21	43	179	6	3.64
SM3	70.08	0.48	14.85	3.00	0.05	0.95	2.07	2.97	4.25	0.14	0.95	99.79	28	38	207	130	22	43	173		
SM4	69.98	0.53	14.90	3.31	0.07	1.12	1.92	2.89	4.86	0.10	0.49	100.17	37	37	232	137	26	42	187		
SM5	69.44	0.50	14.73	3.35	0.00	1.23	2.12	3.38	4.83	0.14	0.55	100.27	28	37	237	142	20	49	181		
SM6	70.08	0.51	14.89	3.23	0.05	1.15	2.03	3.10	5.04	0.13	0.49	100.70	30	37	248	137	21	42	177		

A-type granites. Most of the granites are peraluminous with A/CNK ratios in the range 0.92 to 1.2 (Fig. 3) and so are aluminous A-types in the terminology of King *et al.* (1997). The strongly peraluminous character of the two samples from Oetmoed (A/CNK >1.2, Fig. 3) analysed by Jung *et al.* (1998) reflect their low CaO and Na₂O contents (<1.35 and <2.2 wt.% respectively), rather than unusually high Al₂O₃ contents.

Trace element data

Sr contents decrease with increasing SiO₂ (Fig. 2e) and the samples with >75 wt.% SiO₂ have low Sr contents (<10 ppm in the Dachsberg granite and <30 ppm in many of the Horebis River samples). Many of the less silicic Damara A-type granites have Sr contents that are higher than those of average A-type granites. For example, some samples from the Oetmoed granite with >72 wt.% SiO₂ (Jung *et al.*, 1998) contain >200 ppm Sr, more than double that in the Topsails suite at similar silica values (Fig. 2e). Rb fails to define clear trends when plotted against silica or TiO₂ (not shown) but does become compatible in the highly differentiated Dachsberg granite. Rb/Sr ratios are highest in the Dachsberg (9-28) and Horebis River granites (2.4-10.1).

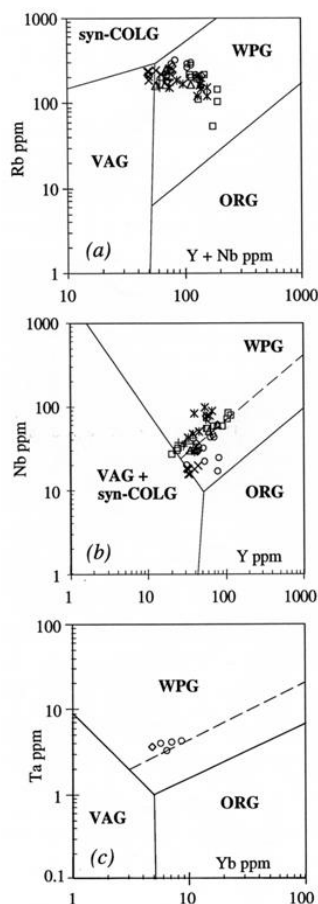


Figure 4: Trace element diagrams (after Pearce *et al.*, 1984) illustrating that all of the A-type granites discussed here are so-called “within-plate” granites and are characterised by HFS element enrichments. Data symbols as in Figure 2.

Most of the samples analysed plot in the within-plate granite fields on Rb vs. Y+Nb, Nb vs. Y and Ta vs. Yb discrimination diagrams (Pearce *et al.*, 1984), (Figs 4a-4c). On a Nb-Y-Ce triangular plot (Eby, 1992) samples from the Horebis River granite plot in the A₁ field while most of the other Damara A-type granites for which these trace element data are available plot in the A₂ field, reflecting lower Nb/Y ratios (Fig. 5). However, the well characterised A-type granite suites from Newfoundland (Whalen *et al.*, 1996) and Padthaway Ridge, South Australia (Turner *et al.*, 1992) which have been interpreted as fractionates from mantle-derived melts also plot in the A₂ field, suggesting that these trace element ratios are not diagnostic of the granitoid sources (see below).

In the Damara A-type granites, Zr contents vary from 94 ppm in the Sorris-Sorris sample with the highest silica content (65.26 wt.% SiO₂, Table 1) to more than 900 ppm in the Albrechtal sample with lowest silica (60.57 wt.% SiO₂, Jung *et al.*, 1997). In all cases zirconium behaves compatibly, indicating zircon crystallisation and removal from zirconium-saturated magmas.

Rare earth element (REE) data for selected A-type granites (Sorris-Sorris, Horebis River and Swakopmund Salem-type granites) exhibit high total REE contents

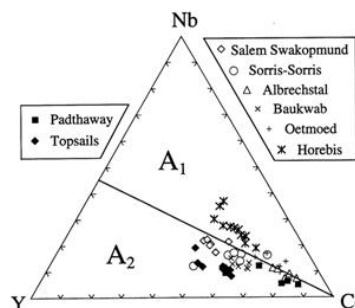


Figure 5: Triangular Nb-Y-Ce diagram after Eby (1992) illustrating the diversity in trace element ratios among different A-type suites from the Damara belt. Also shown are data from well characterised A-type granites from the Topsails suite (Newfoundland, Whalen *et al.*, 1987) and the Padthaway Ridge suite (S. Australia, Turner *et al.*, 1992).

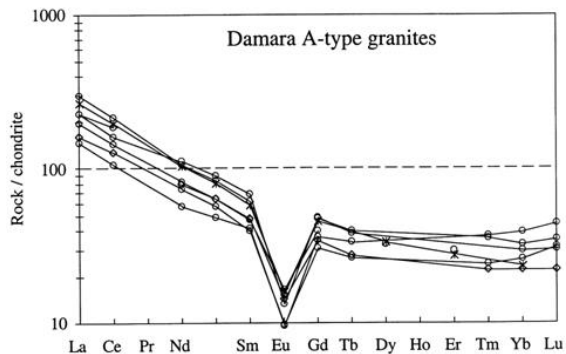


Figure 6: Chondrite normalised REE plots for the Damara A-type granites. Data are given in Table 3. Symbols as in Figure 2.

(Table 2), negative Eu anomalies ($\text{Eu}/\text{Eu}^* = 0.23\text{--}0.39$), high HREE contents and relatively low LREE/HREE ratios ($\text{La}_n/\text{Yb}_n = 3.8\text{--}11.4$, Fig. 6).

Radiogenic Isotope data

ϵ^{Nd} and ϵ^{Sr} values for selected samples, calculated for the time of intrusion of each granitoid, are plotted in Figure 7. Also shown are recently published data from Jung *et al.* (1998) for the HFSE enriched granites from Albrechtstal, Oetmoed and Baukwab (Fig. 1). Data fields for the other Damara granitoid types (Groups I and III, McDermott *et al.*, 1996) are shown for comparison. The data exhibit a restricted range in ϵ^{Sr} and

most granites also have a limited range in ϵ^{Nd} . However, samples from the Sorris-Sorris granite exhibit a wide range in ϵ^{Nd} (-3.3 to -16.4). Most of the Damara A-type granites have ϵ^{Sr} and ϵ^{Nd} values (Fig. 7) that overlap with those from the calc-alkaline Group III granites (diorites and granodiorites) but are distinct from the leucogranites (McDermott, 1986).

In general ϵ^{Nd} in the Sorris-Sorris suite does not correlate with trace element ratios that might be indicative of increased crustal contributions in the samples with lower ϵ^{Nd} (e.g. Rb/Sr, Rb/Ba). However, the Sorris-Sorris samples with highest ϵ^{Nd} have high Nb/Y ratios (Fig. 7 inset) largely reflecting high Nb rather than low Y in the high ϵ^{Nd} samples.

Table 2: REE data for selected HFSE-enriched Damara granitoids

	SM2	YC7	RM 663	RM 664	RM 666	RM 673	RM654
La	53.71	88.10	50.10	64.54	75.92	98.36	74.80
Ce	111.60	172.00	97.74	125.64	163.30	188.00	141.00
Nd	49.97	66.00	36.46	46.93	71.17	67.25	51.70
Sm	9.69	11.80	8.03	8.03	14.01	12.57	9.48
Eu	1.11	1.24	0.70	0.75	1.04	1.20	1.29
Gd	-	10.91	-	-	-	-	9.02
Tb	1.33	-	1.59	1.29	1.83	1.93	-
Dy	-	10.20	-	-	-	-	9.74
Er	-	5.58	-	-	-	-	5.97
Tm	0.67	-	1.19	0.73	-	1.08	-
Yb	4.88	5.18	8.63	5.75	6.55	7.13	5.76
Lu	0.75	-	1.51	1.07	1.02	1.18	-
Eu/Eu*	0.35	0.31	0.25	0.28	0.23	0.28	0.39

Sample SM2 = Swakopmund Salem-type, YC7 = Horebis red granite, RM series samples = Sorris Sorris granite. Dashes denote that element has not been measured. REEs in YC7 and RM654 measured by isotope dilution, all other samples measured by INAA.

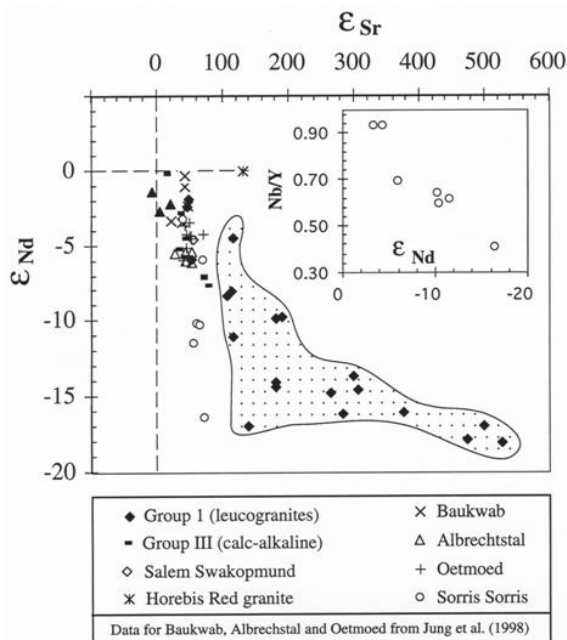


Figure 7: ϵ^{Nd} vs. ϵ^{Sr} (calculated to the intrusion age of each granite) showing the data for A-type Damara granites (*sensu lato*) (Table 3 and Jung *et al.*, 1998). Also shown for comparison is the data field for the so-called Group I granites (leucogranites derived predominantly by partial melting of metasedimentary sources) and the available data for Damara Group III granites (*sensu lato*, predominantly calc-alkaline diorites and quartz diorites).

Discussion

Some models for the genesis of metaluminous to mildly peraluminous A-type granites invoke high-temperature melting of a residual granulitic lower crust from which a felsic melt had been extracted previously (e.g. Collins *et al.*, 1982; Clemens *et al.*, 1986; Whalen *et al.*, 1987; Landenberger and Collins, 1996).

However, there are compelling arguments that the "residual source" model cannot readily explain the enrichment of alkalis over alumina that characterises many A-type suites. These arguments centre on the paucity of alkali feldspar and quartz in granulitic source rocks, and are supported by experimental results. Thus, Creaser *et al.* (1991) compiled data on the mineralogy of residues after experimental melting of amphibolite (Wolf and Wyllie, 1989) and felsic igneous rocks (Conrad *et al.*, 1988, Rutter and Wyllie, 1988) at lower crustal pressures (10 kbar) in order to assess their suitability as sources of A-type granites. Residual assemblages comprised amphibole, clinopyroxene, orthopyroxene, plagioclase \pm opaque minerals and garnet, and so were devoid of the required potassic phases such as alkali-feldspar or biotite. Recent experimental data (Patiño Douce and Beard, 1995, 1996) support these arguments and indicate that granulitic residues remaining after felsic granitic melt extraction have low alkali/alumina ratios and low TiO_2/MgO ratios, the opposite to those observed in most A-type granites.

Alternative models envisage the generation of metaluminous to mildly peraluminous A-type granites by partial melting of H_2O -poor calc-alkaline felsic igneous rocks (Sylvester, 1989; Creaser *et al.*, 1991). Experimental studies have demonstrated that liquids with major element characteristics similar to those of A-type granites can be generated by vapour-absent melting of biotite and amphibole-bearing tonalitic gneiss at pressures of 6-10 kbar (Skjerlie and Johnston, 1992, 1993), although in these experiments the melts typically had higher alumina contents than those commonly observed in A-type granites. More recent dehydration melting experiments on two felsic calc-alkaline rocks, a tonalite and a granodiorite (Patiño Douce, 1997) are in general

agreement with these results but the role of pressure in controlling plagioclase crystallisation was emphasised in the latter study. Selected major element data for the experimental melts produced during Patiño Douce's (1997) experiments are plotted as large symbols on Figure 2. At low pressures (<4 kbar), profuse crystallisation of plagioclase and orthopyroxene accompanies incongruent dehydration melting of calc-alkaline tonalites and granodiorites (open circles and squares respectively, Fig. 2), and this was offered as a mechanism to generate melts with the low Al_2O_3 , CaO and Sr contents of A-type granites (Patiño Douce, 1997). At higher pressures (>8 kbar) the residual mineral assemblage produced during dehydration melting of the same calc-alkaline rocks is dominated by clinopyroxene, with little or no plagioclase crystallisation resulting in higher Al_2O_3 (stipple-filled large circle and square, Fig. 2c). These experiments strongly suggest that typical A-type magmas (with Al, Ca and Sr depletions) may be produced by low-pressure (mid-crustal), but not high-pressure (base of crust), dehydration melting of felsic calc-alkaline rocks. This is our preferred model for the generation of many of the Damara A-type granites with silica contents in the range of about 73-75 wt%. It is important to note that high temperatures (c. 900°C) are required to generate significant melt fractions from water-poor felsic calc-alkaline rocks. Thus, the high magmatic temperatures inferred for many A-type granites and consequent HFS element enrichment do not require a depleted residual source (Creaser *et al.*, 1991; Patiño Douce, 1997).

How might intraplate trace element signatures arise from partial melting of felsic calc-alkaline source rocks? Two explanations are possible. In the first, alluded to above, the higher magmatic temperatures of

A-type magmas promote dissolution of HFS-enriched phases (Watson and Harrison, 1984; Montel, 1993). In the second, halogens play an important role by forming strong complexes with HFS elements (Harris *et al.*, 1986) thereby increasing the HFS element content of the melt relative to the large ion lithophile elements. In order to evaluate the evidence for higher magmatic temperatures compared with those of typical Damara leucogranites, we have calculated the temperatures at which the zirconium and LREE contents of each sample are in equilibrium with zircon and monazite respectively. We note that felsic (but not mafic) crustal protoliths typically contain sufficient Zr and LREE to saturate a peraluminous melt (Watson, 1979; Miller and Mittlefehldt, 1982; Rapp and Watson, 1986). The amount of Zr and LREE that can be accommodated depends upon melt temperature, melt composition, halogen activity and, in the case of monazite solubility, water content (Harrison and Watson, 1983; Watson and Harrison, 1984; Montel, 1993).

Calculated monazite and zircon solubility temperatures are in broad agreement (± 50 °C) in those Damara A-type samples for which both LREE and Zr data are available. Calculated temperatures are based on solubility data derived from low-F systems and, therefore, are likely to represent maximum temperatures if like many A-type granites, those from the Damara belt are F-rich. In Figure 8, the apparent temperatures are plotted against TiO_2 . At a given TiO_2 content, the A-type granites are displaced to higher temperatures compared with the S-type leucogranites and alaskites (McDermott *et al.*, 1996). A similar pattern is observed if the data are plotted against other indices of differentiation (e.g. silica content, not shown). Thus, if we consider the least fractionated samples (highest TiO_2 contents) from

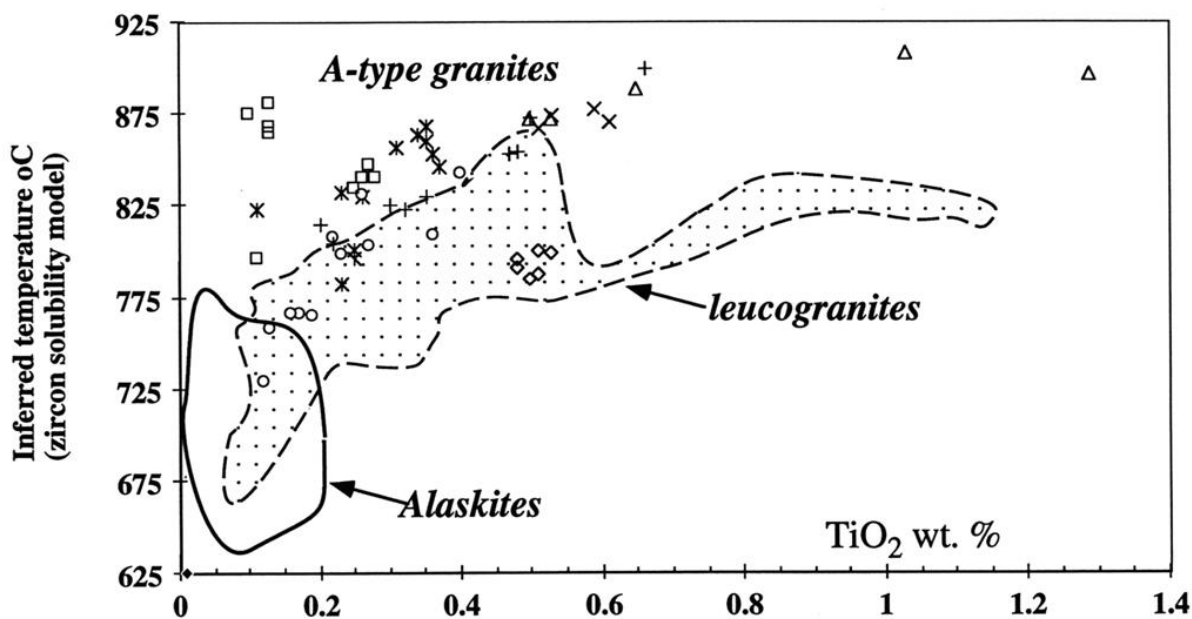


Figure 8: Plot of zircon solubility model temperatures vs. TiO_2 contents. Note that the Damara A-type granites exhibit higher temperatures than S-type leucogranites from the region. Data symbols as in Figure 2.

each granite suite, temperatures inferred from the zircon solubility model are in the range 800 to 910°C for the A-type granites. Leucogranites with similar contents of TiO₂ (and SiO₂, not shown) exhibit systematically lower temperatures, typically in the range 675 to 825°C. The A-type granites studied by Jung *et al.* (1998) tend to be less silicic than those studied here and it is noticeable that they yield high temperatures (c. 880-910°C, see data for Albrechtstal, Baukwab and Oetmoed in Fig. 8). The least evolved sample from the Sorris-Sorris granite yields a temperature of c. 850°C, but the more evolved samples from this granite plot in the field defined by the leucogranite data. Unfortunately no fluorine data are available for these A-type granites, and so we cannot evaluate the extent to which halogen-Zr complexes (e.g. Harris *et al.*, 1986) may have accentuated or even generated the differences in inferred temperatures compared with the leucogranites. In practice it is likely that the two factors are linked because experimental data (Skjerlie and Johnston, 1993) shows that A-type melt generation from F-rich, calc-alkaline source rocks occurs at higher temperatures than from F-poor sources, due largely to the higher thermal stability of F-rich biotite.

The Swakopmund Salem-type granite is unlike the other intrusions discussed here because all six samples plot in the leucogranite field, reflecting low calculated temperatures. Its lower apparent temperatures (reflecting lower zirconium contents) might reflect either (i) derivation from a more mafic crustal source which had insufficient zirconium to saturate the melt and/or (ii) lower F contents. This granite has low FeO_t/(FeO_t+MgO) and TiO₂/MgO ratios (Fig. 2a) and does not strongly exhibit the major element characteristics of A-type granites, yet its Nb and Y contents are relatively high and samples plot consistently in the so-called "within-plate granite" field (Pearce *et al.*, 1984) on trace element discrimination diagrams (Fig. 4).

Some A-type granites are interpreted as the products of extended fractional crystallisation of mantle-derived magmas with insignificant (Turner *et al.*, 1992) or variable degrees of crustal contamination (Kerr and Fryer, 1993; Poitrasson *et al.*, 1995). The highly differentiated nature of the Dachsberg and Horebis River granites probably reflects protracted fractional crystallisation, although the nature of their parental magmas is difficult to constrain. The Dachsberg intrusion is a single feldspar (hypersolvus) granite, which as discussed by Turner *et al.* (1992) is consistent with prolonged low-pressure crystallisation of potassic feldspar over a wide temperature interval. These intrusions have the highest Nb contents and highest Nb/Y ratios of any of the Damara A-type granites (*sensu-stricto*). The Horebis River granite plots in the A₁ field of Eby (1992). However, the high ratios are best developed in the highest silica samples (not shown) suggesting that these are not features of the parental magma. One difficulty in evaluating the role of crustal interactions accompanying frac-

tional crystallisation is that their extreme Sr depletion as a result of feldspar fractional crystallisation (typically <20 ppm Sr in the Dachsberg samples), renders their Sr isotope ratios highly sensitive to change as a result of interaction with more radiogenic crustal rocks. In this regard we note that the two Damara A-type granites with highest initial ⁸⁷Sr/⁸⁶Sr ratios (Horebis River and Dachsberg) also have the lowest Sr contents.

In contrast with these high-silica granites, several Damara A-type granites (Albrechtstal, Baukwab, Oetmoed) exhibit silica values (60-69 wt.% SiO₂) that are lower than those in melts generated by experimental partial melting of tonalites and granodiorites, (74 ± 1.5 wt.% SiO₂, Patiño Douce, 1997, see Fig. 2). The low silica contents of the Albrechtstal, Baukwab and Oetmoed granites contrast with, for example, the high silica contents (>70 wt.%) of the Lachlan Fold Belt A-type granite intrusions discussed by King *et al.* (1997). The latter were interpreted as high-temperature melts of felsic crustal sources, consistent with the experimental data discussed above. In view of the requirement to produce magmas with lower silica values than those of typical A-type granites, we concur with Jung *et al.* (1998) who, on the basis of their isotope data, interpreted these lower silica A-type granites as mixed sources involving juvenile mantle-derived and crustal rocks.

Conclusions

The Damara A-type granites exhibit a wide compositional range and vary from low silica examples (the Albrechtstal granite) to highly fractionated, high-silica granites (Dachsberg and Horebis River granites). The restricted range in initial ⁸⁷Sr/⁸⁶Sr in most of the A-type granites precludes significant involvement of old (pre-Damara) high Rb/Sr, upper crustal granitic or meta-sedimentary sources. The parental magmas for several of the Damara A-type granites (Sorris-Sorris, Horebis River, Dachsberg) may have been generated by high-temperature, low-pressure (mid-crustal) partial melting of felsic calc-alkaline source rocks. With the exception of the Sorris-Sorris granite, the Damara A-type granites exhibit a narrow range in εNd_t indicating derivation from juvenile crustal sources. Early diorites and granodiorites intruded during the Damara orogeny exhibit similar isotopic characteristics and are plausible source materials for the post-tectonic A-type granites. While models that require some coeval contributions from mantle sources are difficult to rule out, a major role for felsic crustal lithologies as sources seems inescapable in view of the observation that sufficient zirconium was available to saturate the melts, and so yield high zircon solubility temperatures. By contrast, some A-type granites (Albrechtstal, Oetmoed and Baukwab) have lower silica contents and higher TiO₂, MgO, CaO and total Fe (Jung *et al.*, 1998) than those typically generated in melting experiments on felsic calc-alkaline source rocks. These probably require more mafic source rocks to generate

the observed low silica, high CaO and high Sr contents. Nevertheless, their sources probably contained some felsic crustal lithologies in order to provide sufficient zirconium to saturate the melts and so yield high zircon and monazite saturation temperatures. As discussed by Jung *et al.* (1998), such a mixed-source rather than crustal assimilation by a mantle-derived magma is consistent with their trace element, radiogenic and stable isotope data.

In summary, we tentatively conclude that some of the lower silica Damara A-type granites preserve evidence for the involvement of mafic sources, in marked contrast with the more voluminous S-type leucogranites that dominate the orogenic belt. However, many of the Damara A-type granites have major element, trace element and radiogenic isotope data that are consistent with derivation by low-pressure, intracrustal melting of felsic calc-alkaline rocks. Their relatively old Nd models ages (typically mid-Proterozoic, Table 3) appear to preclude significant involvement of contemporaneous juvenile mantle-derived material. An important unresolved issue is the heat source required to generate hot magmas (>800°C at mid-crustal levels). If heat was transferred into the lower to middle crust primarily by conduction in response to basalt underplating, little or no mass-transfer to the crust is required. However, in a recent re-appraisal of the Ivrea zone (southern Alps, northern Italy) Barboza *et al.* (1999) demonstrated that regional high-grade metamorphism pre-dated the intrusion of mafic magma into the lower crust, implying that emplacement of basaltic magma into the base of the crust does not necessarily cause large-scale anatexis. If, as seems more likely, heat was advected to the middle crust by upwelling of hot asthenospheric material, crustal growth estimates based on the present erosion level could underestimate of the amount of new material added to the crust during the Damara Orogeny.

Acknowledgements

The manuscript was improved by constructive comments from reviews by Drs Mike Brown and Fernando Bea. The authors gratefully acknowledge the superb lo-

gistical support provided by Dr Roy Miller, Director of the Geological Survey of Namibia in Windhoek when fieldwork was undertaken in the mid-1980s. Alan Marlow and Kevin Downing supplied some of the granite samples. Nick Rogers provided the INAA data. Peter van Calsteren is thanked for his help with the isotope measurements. Peter Webb and John Watson assisted with the XRF analyses. This study formed part of an Open University funded Ph.D. studentship which FMcD gratefully acknowledges.

References

- Barboza, S.A., Bergantz, G.W. and Brown, M. 1999. Regional granulite facies metamorphism in the Ivrea zone: Is the Mafic Complex the smoking gun or a red herring? *Geology*, **27**, 447-450.
- Collins, W.J., Beams, S.D. and White, A.J.R. 1982. Nature and origin of A-type granites with particular reference to south-eastern Australia. *Contrib. Mineral. Petrol.*, **80**, 189-200.
- Conrad, W.K., Nicholls, I.A. and Wall, V.J. 1988. Water-saturated and undersaturated melting of metaluminous and peraluminous crustal compositions at 10 kb: Evidence for the origin of silicic magmas in the Taupo Volcanic Zone, New Zealand, and other occurrences. *J. Petrol.*, **29**, 765-803.
- Clemens, J.D., Holloway, J.R. and White, A.J.R. 1986. Origin of an A-type granite: Experimental constraints. *Am. Miner.*, **71**, 317-324.
- Creaser, R.A. and White, A.J.R. 1991. Yardea Dacite - Large-volume, high-temperature felsic volcanism from the Middle Proterozoic of South Australia. *Geology*, **19**, 48-51.
- Creaser, R.A., Price, R.C. and Wormald, R.J. 1991. A-type granites revisited: Assessment of a residual-source model. *Geology*, **19**, 163-166.
- Downing, K.N. and Coward, M.P. 1981. The Okahandja lineament and its significance for Damaran tectonics in Namibia. *Geol. Rdsch.*, **70**, 9721-1000.
- Eby, G.N. 1992. Chemical subdivision of the A-type granitoids: Petrogenetic and tectonic implications. *Geology*, **20**, 641-644.

Table 3: Sr and Nd isotope data for selected Damara HFSE-enriched granitoids.

Sample	Age (Myr)	¹⁴³ Nd/ ¹⁴⁴ Nd (present)	Nd	Sm	¹⁴⁷ Sm/ ¹⁴⁴ Nd	TNd _{DM} (Gyr)	ε _{Nd(t)}	Rb ppm	Sr ppm	⁸⁷ Sr/ ⁸⁶ Sr (present)	⁸⁷ Rb/ ⁸⁶ Sr	⁸⁷ Sr/ ⁸⁶ Sr	ε _{Sr}
Swakopmund Salem-type granite													
SM2	563±63	0.51211	50	9.69	0.12	1.44	-4.59	186	132	0.74077	4.092	0.70793	55.52
Horebis red granite													
Yc7	633±39	0.51227	66	11.8	0.11	1.13	-0.01	143	53	0.78465	7.868	0.71361	137.42
Sorris-Sorris granite													
RM 654	495±15	0.51152	51.7	9.48	0.11	2.28	-16.40	240	167	0.73855	4.172	0.70912	71.28
RM 662	495±15	0.51176	101	14.5	0.09	1.53	-10.19	219	213	0.72941	2.982	0.70837	60.67
RM 664	495±15	0.51175	46.9	8.03	0.10	2.06	-11.44	321	98	0.77542	9.543	0.70810	56.84
RM 666	495±15	0.51208	71.2	14.01	0.12	1.65	-5.98	232	106	0.75384	6.363	0.70895	68.91
RM 673	495±15	0.51184	67.3	12.57	0.11	1.92	-10.29	279	117	0.75756	6.936	0.70864	64.42
Sor 2203	495±15	0.51209	98.7	15.32	0.09	1.21	-4.19	215	131	0.76039	4.775	0.72671	321.02
Sor 2204	495±15	0.51215	80.4	13.00	0.10	1.18	-3.27	216	134	0.73983	4.680	0.70681	38.50

- Esquevin, J. and Menendez, R. 1974. *Age Rb/Sr des granites du permies Diana (Omakuara et Sandflats, S.W.A.)*. Unpubl. S.N.P.A. report for Aquitaine S.W.A., Mineral Exploration, 14 pp.
- Haack, U., Hoefs, J. and Gohn, E. 1982. Constraints on the origin of Damaran granites by Rb/Sr and $\delta^{18}\text{O}$ data. *Contrib. Mineral. Petrol.*, **79**, 279-289.
- Harris, N.B.W., Marzouki, F.M.H. and Ali, S. 1986. The Jabel Sayid complex, Arabian Shield: geochemical constraints on the origin of peralkaline and related granites. *J. geol. Soc. London*, **143**, 287-295.
- Harris, N.B.W., Hawkesworth, C.J. and McDermott, F. 1987. Evolution of continental crust in southern Africa. *Earth Planet. Sci. Lett.*, **83**, 85-93.
- Harrison, T.M. and Watson, E.B. 1983. Kinetics of zircon dissolution and zirconium diffusion in granitic melts of variable water content. *Contrib. Mineral. Petrol.*, **84**, 66-72.
- Hawkesworth, C.J., Kramers, K.D. and Miller, R.McG. 1981. Old model Nd ages in Namibian Pan-African rocks. *Nature*, **289**, 278-282.
- Hawkesworth, C.J. and Marlow, A.G. 1983. Isotope evolution of the Damara Orogenic Belt, 397-407. In: Miller, R.McG. (ed.) *Evolution of the Damara orogen of South West Africa/Namibia*. Spec. Publ. geol. Soc. S. Afr., **11**, 515 pp.
- Hawkesworth, C.J., Gledhill, A.R., Roddick, J.C., Miller R. McG. and Kröner, A. 1983. Rb-Sr and $^{40}\text{Ar}/^{39}\text{Ar}$ studies bearing on models for the thermal evolution of the Damara Belt, Namibia, 323-338. In: Miller, R.McG. (ed.) *Evolution of the Damara Orogen of South West Africa/Namibia*. Spec. Publ. geol. Soc. S. Afr., **11**, 515 pp.
- Jung, S., Mezger, K. and Hoernes, S. 1998. Petrology and geochemistry of syn- to post-collisional metaluminous A-type granites - a major and trace element and Nd-Sr-Pb-O-isotope study from the Proterozoic Damara Belt, Namibia. *Lithos*, **45**, 147-175.
- Kerr, A. and Fryer, B.J. 1993. Nd isotopic evidence for crust-mantle interaction in the generation of A-type granitoid suites in Labrador, Canada. *Chem. Geol.*, **104**, 39-60.
- King, P.L., White, A.J.R., Chappell, B.W. and Allen, C.M. 1997. Characterisation and origin of aluminous A-type granites from the Lachlan Fold Belt, Southeastern Australia. *J. Petrol.*, **38**, 371-391.
- Landenberger, B. and Collins, W.J. 1996. Derivation of A-type granites from a dehydrated charnockitic lower crust: Evidence from the Chaelundi Complex, Eastern Australia. *J. Petrol.*, **37**, 145-170.
- Martin, H. and Porada, H. 1977. The intracratonic branch of the Damara Orogen in South West Africa, 1. Discussion of Geodynamic models II. Discussion of relationships with the Pan-African Mobile Belt System. *Precamb. Res.*, **5**, 311-338; 339-357.
- McDermott, F. 1986. *Granite petrogenesis and crustal evolution studies in the Damara Belt, Namibia*. Unpubl. Ph.D. thesis. Open Univ., 303pp.
- McDermott, F., Harris, N.B.W. and Hawkesworth, C.J. 1996. Geochemical constraints on crustal anatexis: a case study from the Pan-African Damara granitoids of Namibia. *Contrib. Mineral. Petrol.*, **123**, 406-423.
- Miller, C.F. and Mittlefehldt, D.W. 1982. Depletion of light rare earth elements in felsic magmas. *Geology*, **10**, 129-133.
- Miller, R.McG. 1980. Geology of a portion of central Damaraland, South West Africa/Namibia. *Mem. geol. Surv. S. Afr. (S.W. Afr. Ser.)*, **6**, 78 pp.
- Miller, R.McG. 1983. The Pan African Damara Orogen of South West Africa/Namibia, 431-515. In: Miller, R.McG. (ed.) *Evolution of the Damara orogen of South West Africa/Namibia*. Spec. Publ. geol. Soc. S. Afr., **11**, 515 pp.
- Montel, J.M. 1993. A model for monazite melt equilibrium and applications to the generation of granitic magmas. *Chem. Geol.*, **110**, 127-146.
- Patiño Douce, A.E. and Beard, J.S. 1995. Dehydration melting of biotite gneiss and quartz amphibolite from 3 to 15 kbar. *J. Petrol.*, **36**, 707-738.
- Patiño Douce, A.E. and Beard, J.S. 1996. Effects of P, f(O₂) and Mg/Fe ratio on dehydration melting of model metagreywackes. *J. Petrol.*, **37**, 999-1024.
- Patiño Douce, A.E. 1997. Generation of metaluminous A-type granites by lower pressure melting of calc-alkaline granitoids. *Geology*, **25**, 743-746.
- Pearce, J.A., Harris, N.B.W. and Tindle, A.G. 1984. Trace element discrimination diagrams for the tectonic interpretation of granitic rocks. *J. Petrol.*, **25**, 956-983.
- Pitcher, W.S. 1979. Comments on the geological environments of granites, 1-8. In: Atherton, M.P. and Tarney, J. (eds) *Origin of Granite Batholiths: Geochemical Evidence*. Shiva, 148 pp.
- Poitrasson, F., Duthou, J.L. and Pin, C. 1995. The relationship between petrology and Nd isotopes as evidence for contrasting anorogenic granite genesis: Example of the Corsican Province (SE France). *J. Petrol.*, **36**, 1251-1274.
- Rapp, R.P. and Watson, E.B. 1986. Monazite solubility and dissolution kinetics: implications for the thorium and light rare earth chemistry of felsic magmas. *Contrib. Mineral. Petrol.*, **94**, 304-316.
- Rutter, M.J. and Wyllie, P.J. 1988. Melting of vapour-absent tonalite at 10 kbar to simulate dehydration melting in the deep crust. *Nature*, **331**, 159-160.
- Skjerlie, K.P. and Johnston, A.D. 1992. Vapour-absent melting at 10 kbar of a biotite- and amphibole-bearing tonalite gneiss: implications for the generation of A-type granites. *Geology*, **20**, 263-266.
- Skjerlie, K.P. and Johnston, A.D. 1993. Fluid-absent melting behaviour of a F-rich tonalitic gneiss at mid-crustal pressures: implications for the generation of anorogenic granites. *J. Petrol.*, **34**, 785-815.
- Sylvester, P.J. 1989. Post-collisional alkaline granites. *J. Geol.*, **97**, 261-280.

- Turner, S.P., Foden, J.D. and Morrison, R.S. 1992. Derivation of A-type magmas by fractionation of basaltic magma: an example from the Padthaway Ridge, South Australia. *Lithos*, **28**, 151-179.
- Watson, E.B. 1979. Zircon saturation in felsic liquids: Experimental results and applications to trace element geochemistry. *Contrib. Mineral. Petrol.*, **70**, 407-419.
- Watson, E.B. and Harrison, T.M. 1984. Accessory minerals and the geochemical evolution of crustal magmatic systems: A summary and prospectus of experimental approaches. *Phys. Earth Planet. Interiors.*, **79**, 151-158.
- Whalen, J.B., Currie, K.L. and Chappell, B.W. 1987. A-type granites: geochemical characteristics, discrimination and petrogenesis. *Contrib. Mineral. Petrol.*, **95**, 407-419.
- Whalen, J.B., Jenner, G.A., Longstaffe, F.J., Robert, F. and Gariépy, C. 1996. Geochemical and isotopic (O, Nd, Pb and Sr) constraints on A-type granite petrogenesis based on the Topsails igneous suite, Newfoundland Appalachians. *J. Petrol.*, **37**, 1463-1489.
- White, A.J.R. and Chappell, B.W. 1983. Granitoid types and their distribution in the Lachlan Fold Belt, Southeastern Australia. *Mem. geol. Soc. Am.*, **159**, 21-34.
- Wolf, M.B. and Wyllie, P.J. 1989. The formation of tonalitic liquids during the vapour-absent partial melting of amphibolite at 10 kb. *Abs. Eos Trans. Am. geophys. U.*, **70**, 506.

Appendix 1 - Analytical techniques

Major elements were determined on fused glass discs using an energy dispersive XRF system at the Open University (Link Systems Meca 10-44). Detection limits for the major elements were generally 0.05 wt. % except for the light elements Na, Mg, Al and Si for which detection limits were between 0.2 (Si) and 0.96 wt % (Na). Precision was typically better than 1% relative (2 σ) except for Al (2%), Mg (3%) and Na (10%). Trace elements were determined on pressed powder pellets using a Phillips PW1400 wavelength dispersive XRF spectrometer at Nottingham University. Precision for all trace elements was approximately 2% at the 100 ppm level. The REE, Th, Ta, Hf and U were determined on 0.3g powder samples by instrumental neutron activation analysis (INAA). Full details of the counting conditions, peak fitting, calibration and corrections are described in Potts *et al.* (1985). Rock powders were dissolved in pressurised teflon reaction vessels (bombs) for the Sr and Nd isotope analyses. All dissolutions and chemical separations were performed in a clean-air laboratory, and the total procedural blanks were less than 1ng for both Sr and Nd. Isotope ratios were measured in peak-switching mode using a single collector mass-spectrometer (VG 54E) at the Open University, and the peak intensities were calculated using a double interpolation algorithm. $^{87}\text{Sr}/^{86}\text{Sr}$ ratios were corrected for mass-fractionation using a linear fraction law and a $^{86}\text{Sr}/^{88}\text{Sr}$ ratio of 0.1194 and $^{143}\text{Nd}/^{144}\text{Nd}$ ratios were corrected for mass-fractionation assuming a $^{146}\text{Nd}/^{144}\text{Nd}$ ratio of 0.7219. NBS 987 gave a value of 0.71024 \pm 2 and the Johnston Matthey Nd standard gave a value of 0.511848 \pm 15.

Appendix 2 - Field Descriptions of sampling sites

Field notes on samples collected by F. McDermott in 1984 and 1985.

Dachsberg granite.

Post-tectonic granite. Sampled at farm Sandflats (123) and farm Omakuara (142), Gobabis District. Samples 1010, 1011 from the N. side of the intrusion; samples 1012, 1013 and 1014 from the east side of the intrusion. Sample 1015 from the other distinct koppie to the north of Sandflats. Samples 1030 - 1035 inclusive from the Dachsberg granite on farm Omakuara. (McDermott, 1986).

Sorris-Sorris granite

Post-tectonic granite. Samples 2198-2200 inclusive collected from a single freshly blasted site on north-side of road to farm Sorris-Sorris. Sampled site was 2.5 km along road from the junction that is approximately 3 km north of Uisberge. Sample 2204 is from a roadside blast exposure at Ugab river bridge (farm Onverwag 412) on the main road southwards from Khorixas to Omaruru. RM series samples from Sorris-Sorris collected by R. Miller (see Miller, 1980 and Hawkesworth *et al.*, 1983).